Computers, Materials & Continua

Tech Science Press

Doi:10.32604/cmc.2025.066138

ARTICLE

Optimizing Microgrid Energy Management via DE-HHO Hybrid Metaheuristics

Jingrui Liu[1,2,*], **Zhiwen Hou**[1,2], **Boyu Wang**[1,2] **and Tianxiang Yin**[3,4]

[1]Chongqing University-University of Cincinnati Joint Co-op Institute, Chongqing University, Chongqing, 400044, China
[2]Department of Electrical and Computer Engineering, University of Cincinnati, Cincinnati, OH 45221, USA
[3]National Elite Institute of Engineering, Chongqing University, Chongqing, 401135, China
[4]School of Life Sciences, Chongqing University, Chongqing, 401331, China

*Corresponding Author: Jingrui Liu. Email: liu3jr@mail.uc.edu

Received: 31 March 2025; Accepted: 29 May 2025; Published: 30 July 2025

ABSTRACT: In response to the increasing global energy demand and environmental pollution, microgrids have emerged as an innovative solution by integrating distributed energy resources (DERs), energy storage systems, and loads to improve energy efficiency and reliability. This study proposes a novel hybrid optimization algorithm, DE-HHO, combining differential evolution (DE) and Harris Hawks optimization (HHO) to address microgrid scheduling issues. The proposed method adopts a multi-objective optimization framework that simultaneously minimizes operational costs and environmental impacts. The DE-HHO algorithm demonstrates significant advantages in convergence speed and global search capability through the analysis of wind, solar, micro-gas turbine, and battery models. Comprehensive simulation tests show that DE-HHO converges rapidly within 10 iterations and achieves a 4.5% reduction in total cost compared to PSO and a 5.4% reduction compared to HHO. Specifically, DE-HHO attains an optimal total cost of $20,221.37, outperforming PSO ($21,184.45) and HHO ($21,372.24). The maximum cost obtained by DE-HHO is $23,420.55, with a mean of $21,615.77, indicating stability and cost control capabilities. These results highlight the effectiveness of DE-HHO in reducing operational costs and enhancing system stability for efficient and sustainable microgrid operation.

KEYWORDS: Microgrid optimization; differential evolution; Harris Hawks optimization; multi-objective scheduling

1 Introduction

With the global demand for energy steadily increasing, the depletion of traditional fossil fuel resources and worsening environmental pollution have presented significant challenges to power grid systems [1]. Conventional grids, which depend heavily on large-scale centralized generation and long-distance transmission, suffer from low energy efficiency. Additionally, they are vulnerable to natural disasters and equipment failures, compromising the reliability of power supply [2,3].

Microgrids, as an innovative power system, are composed of distributed generation (DG), energy storage systems, and loads, and can operate flexibly in both grid-connected and islanded modes [4]. They enable the effective integration and utilization of clean energy sources such as wind and solar power, while leveraging energy storage systems to smooth energy fluctuations and ensure stable and reliable electricity supply [5–7]. The advantages of microgrids in various aspects are shown in Table 1 [8,9].

Table 1: Advantages of microgrids in various aspects

Energy efficiency	Power supply reliability	Sustainability	Flexibility
By generating power locally and consuming it on-site, microgrids minimize transmission losses and enhance energy utilization efficiency.	Microgrids have the capability to operate autonomously when disconnected from the main grid, ensuring a stable power supply for critical loads.	By integrating clean energy sources and implementing efficiency enhancements, microgrids contribute to the reduction of greenhouse gas emissions and other pollutants.	Microgrids can be customized and scaled to meet the specific needs of diverse application scenarios and load demands.

Energy optimization scheduling in microgrids involves coordinating the output of distributed energy resources and managing energy exchange between the microgrid and the main grid under various system constraints [10]. This process seeks to achieve multiple objectives, including minimizing operational costs and emissions, improving reliability, and enhancing energy efficiency [11]. From the demand-side perspective, optimized scheduling reduces electricity costs for consumers. From the supply-side perspective, it improves grid stability, decreases generation-related energy losses, and mitigates environmental pollution [12].

Given the increasing penetration of renewable energy sources and the challenges posed by their inherent variability and intermittency, energy optimization in microgrid scheduling has emerged as a critical research focus. This study seeks to explore advanced scheduling strategies and optimization methods to address these challenges, ensuring the efficient, economical, and sustainable operation of microgrid systems. The findings are expected to contribute to a broader transition toward greener and more resilient energy systems.

The configuration and optimization of energy storage (ES) systems have long been a major research focus in the context of microgrids [13]. Nayak et al. [14] employed probabilistic and statistical methods to analyze system output characteristics and developed mathematical probability models to determine ES capacity allocation and reliability metrics. However, these models exhibited significant stochasticity, leading to discrepancies between simulation results and actual data. Sultan et al. [15] proposed an economic model to optimize ES capacity under system output fluctuations, yet these approaches lacked specificity for different ES types and relied on relatively simplistic economic frameworks.

To address these limitations, Wang et al. [16] developed an optimization model aimed at minimizing the variance of load fluctuations, thereby effectively improving the voltage stability and economic efficiency of distribution networks. However, these studies overlooked critical ES characteristics, focusing primarily on the isolated aspects of energy storage without fully addressing the integration and synergy of multiple energy resources. The lack of a comprehensive approach limits the applicability of these models in real-world scenarios, where effective management of different energy systems is crucial. To overcome these challenges, recent research has shifted toward exploring microgrid configurations that integrate various energy resources through advanced Energy Management Systems (EMS) and optimization techniques. For instance, Mehleri et al. utilized a mixed-integer nonlinear programming (MINLP) method to minimize an objective function that includes investment, operation, maintenance, and environmental costs [17]. Although MINLP provides

a systematic framework for microgrid optimization, its application in large-scale nonlinear problems is constrained by computational inefficiency.

As a result, many researchers have adopted intelligent optimization algorithms to solve microgrid optimization scheduling problems. Among these, particle swarm optimization (PSO) has been widely applied due to its simplicity and ease of implementation. For example, Abood et al. proposed a novel energy management method called accelerated PSO [18]. Abualigah et al. and Zermane et al. [19,20] developed quantitative models for battery lifespan in ES systems and solved these models using PSO. Additionally, Guo et al. designed an ES system model with economic indicators and achieved optimal solutions through PSO [21].

In addition to the PSO algorithm, researchers have explored various other intelligent optimization methods. For example, Zhao et al. used particle swarms with automatic parameter configuration to optimize hierarchical parallel search [22]. Furthermore, some scholars have proposed intelligent EMS based on Genetic Algorithms (GA), incorporating forecasting modules, energy storage management modules, and optimization modules [23].

However, traditional optimization algorithms exhibit inherent limitations in practical applications, including susceptibility to local optima, limited global search capability, slow convergence, and constrained applicability [24–28]. To address these shortcomings, the HHO algorithm has recently emerged as a promising solution for microgrid optimization problems [29]. Inspired by the cooperative hunting behavior of Harris hawks, HHO is notable for its simplicity, low parameter dependence, and ease of implementation. It has been successfully applied in various fields, including numerical and engineering optimization, image recognition, fault diagnosis, and power grid optimization design [30]. To further improve optimization performance, researchers have integrated HHO with the Differential Evolution (DE) algorithm [31]. DE employs differential mutation and crossover operations, using the differences among individuals in the population to generate new candidate solutions. This method is conceptually simple, requires few control parameters, and demonstrates strong robustness [32]. By combining the global search capability of DE with the local exploitation strength of HHO, the hybrid DE-HHO algorithm significantly improves convergence speed, enhances global search efficiency, and effectively avoids entrapment in local optima.

This study focuses on optimizing the scheduling of a microgrid comprising wind, solar, and energy storage systems, with the objective of minimizing both operational and maintenance costs as well as environmental economic costs. A comprehensive optimization model is developed, incorporating mathematical representations of each component and defining relevant constraints to analyze the energy consumption of critical loads within the microgrid. The hybrid DE-HHO algorithm is employed to solve the model, determining the optimal output of each component to minimize total cost. Finally, case studies are conducted to verify the feasibility and effectiveness of the proposed algorithm.

The contributions of this study are summarized as follows:

- A hybrid optimization algorithm, DE-HHO, is proposed, which combines the global search capability of DE and the local exploitation capability of HHO. This algorithm noticeably enhances the convergence speed and stability of microgrid scheduling and effectively reduces operational costs.
- A multi-objective optimization model for microgrids is constructed, covering wind, solar, micro-gas turbine, and energy storage systems. This model considers both operational costs and environmental impacts, ensuring the stability and reliability of the system.
- The effectiveness of the DE-HHO algorithm is verified through simulation experiments. The results show that the algorithm can effectively reduce operational costs and optimize energy dispatch strategies for microgrids.

The rest of this paper is organized as follows: Section 2 introduces the modeling of microgrids with wind, solar, micro-gas turbine, and energy storage systems. Section 3 presents the operational optimization strategies for microgrids. Section 4 elaborates on the design and implementation of the DE-HHO hybrid optimization algorithm. Section 5 demonstrates the simulation results and analysis. Finally, Section 6 summarizes the research findings and proposes future research directions.

2 System Models

Microgenerators are renewable or unconventional power generation units integrated within microgrids, commonly referred to as DERs. The application of microgenerators is anticipated to expand significantly in the future [33]. In a microgrid, these power sources not only provide electrical energy to the system but also play a pivotal role in ensuring system stability and maintaining power quality. This study examines several common types of microgenerators, including wind turbines, photovoltaic (PV) systems, micro gas turbines, and energy storage batteries, as shown in Fig. 1. The subsequent sections provide an analysis of the output models for each of these four microgeneration technologies.

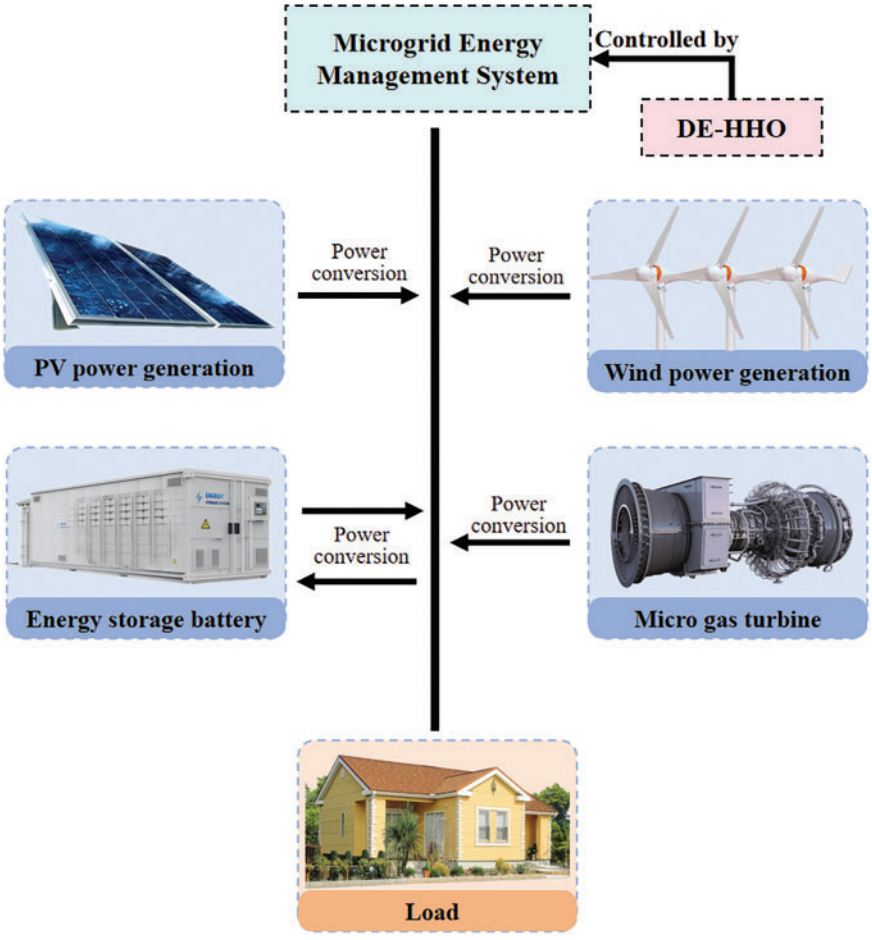

Figure 1: A microgrid with an EMS

2.1 Wind Power Generation Modeling

The principle of wind power generation involves converting natural wind energy into usable electrical energy through wind turbines (WT) [34]. As a form of renewable energy, wind power is environmentally friendly and does not consume any fuel. However, the inherent randomness of natural wind makes it challenging to precisely predict the output of wind power generation.

The following section presents an analysis of widely applied wind power generation models, along with the calculation formula for wind power output P_{wind}.

$$P_{wind} = \begin{cases} 0 & 0 \le v \le V_{in}, v \ge V_{out} \\ P_0 & V_o \le v \le V_{out} \\ h(v) & V_{in} \le v \le V_o \end{cases} \tag{1}$$

In Eq. (1), v represents the real-time wind speed; V_{in} denotes the cut-in wind speed of the turbine; V_{out} is the cut-out wind speed; V_o indicates the rated wind speed of the turbine; and P_o represents the rated output power of the turbine. When the real-time wind speed lies between the cut-in and rated wind speeds, the relationship between the turbine's output power and the real-time wind speed can be expressed as $h(v)$:

$$h(v) = k_2 \cdot v^2 + k_1 \cdot v + k_0 \tag{2}$$

In the equation, k_0, k_1, and k_2 represent the characteristic parameters of the wind turbine.

The operating states of the wind turbine can be summarized into the following three cases:

1. No Power Generation: When $0 \le v \le V_{in}, v \ge V_{out}$, the turbine does not generate power as the real-time wind speed is below the cut-in speed or above the cut-out speed.

2. Rated Power Generation: When $V_o \le v \le V_{out}$, the turbine generates power equal to its rated output power.

3. Variable Power Generation: When $V_{in} \le v \le V_o$, the turbine's output power follows a functional relationship as defined in Eq. (2).

2.2 Photovoltaic (PV) Power Generation Modeling

The fundamental principle of photovoltaic (PV) power generation involves the absorption of solar energy by PV modules, which convert it into electricity for practical use. As the process requires no fuel consumption, PV power generation effectively eliminates emissions associated with fossil fuel combustion, thereby reducing air pollution and mitigating the greenhouse effect.

A PV power generation system consists primarily of PV modules that absorb solar radiation and generate direct current (DC) electricity. Since PV modules output DC power while most electrical grids and devices operate on alternating current (AC), a DC-to-AC conversion is necessary to adapt the generated electricity. Energy storage devices are used to store excess electricity produced during periods of low demand, which is particularly critical in large-scale PV power plants to ensure a stable power supply. The configuration of PV cells, whether in series or parallel, enables flexible adjustment of system voltage and current to optimize power output. By employing advanced inverter control strategies, Maximum Power Point Tracking (MPPT) can be achieved to maximize energy utilization. Additionally, optimizing the tilt angle of the PV panels further enhances generation efficiency [35].

The output power of a PV system P_{pv} is strongly influenced by solar irradiance and ambient temperature, and its performance can be described using the mathematical expression provided in Eq. (3).

$$P_{pv} = \eta_{pv} \cdot n \cdot S \cdot I \left(1 - \varpi \left(T - T_{base}\right)\right) \tag{3}$$

The equation, η_{pv} represents the conversion efficiency of the PV modules; n denotes the number of PV panels; S is the area of each PV panel; I represents the solar irradiance; ϖ is the temperature sensitivity coefficient; T refers to the ambient temperature; and T_{base} is the reference temperature, typically set at 25°C.

The operating characteristics of PV power generation can be summarized as follows:

1. In solar cells, photon energy is used to excite electrons, generating current. A higher number of photons (i.e., greater solar irradiance) results in more electrons being excited, thereby producing higher current and power output. Consequently, the greater the solar irradiance, the more solar energy the PV modules can absorb, leading to a higher maximum power output.

2. During operation, PV modules generate heat, and elevated temperatures reduce the efficiency of semiconductor materials, thus diminishing the overall performance of the PV modules. As the temperature increases, the internal resistance of the PV modules may rise, leading to a decrease in their maximum power output.

2.3 Micro Gas Turbines (MGTs) Modeling

Micro Gas Turbines (MGTs) are small-scale, gas-powered devices primarily employed in distributed power generation systems. The core operating principle involves the combustion of natural gas or other fuels to generate high-temperature, high-pressure gases. These gases drive a turbine, which subsequently powers a generator to produce electricity. Compared to conventional large-scale gas turbines, MGTs offer several advantages, including compact size, high efficiency, and rapid response times, making them particularly well-suited for integration into distributed generation systems such as microgrids [36].

The operating mechanism of an MGT involves three key processes: air compression, fuel combustion, and gas expansion. Air is compressed by a compressor, then mixed with fuel and ignited in the combustion chamber to produce high-temperature gases. These gases expand to drive the turbine, which, in turn, converts mechanical energy into electrical energy via a generator.

In microgrids, MGTs are commonly utilized for load regulation and grid stabilization. The mathematical model governing their operation can be expressed by the following equations:

$$P_{GT} = \eta_{GT} \cdot m_{fuel} \left(h_{out} - h_{in}\right) \tag{4}$$

In the equations, P_{GT} represents the output power of the micro gas turbine, m_{fuel} is the fuel flow rate. h_{out} and h_{in} are the enthalpy values of the gas at the inlet and outlet, respectively. Additionally, we have simplified the variations in load and environmental conditions during the operation of the turbine, setting the turbine's efficiency η_{GT} to a constant value to facilitate analysis and calculation. Micro gas turbines generate electricity by consuming fuel, which incurs operational and maintenance (O&M) costs, fuel costs, and pollutant treatment expenses. The mathematical expressions for these costs are detailed as follows:

$$C_o\left(t\right) = \lambda_o \cdot P_{GT}\left(t\right) \tag{5}$$

In the equation, $C_o\left(t\right)$ represents the O&M cost at time t; λ_o denotes the O&M cost coefficient, indicating the cost per unit of power; and Pout, $P_{GT}\left(t\right)$ is the active power output of the micro gas turbine

at time t.

$$C_f(t) = \frac{C_{fuel}}{V_{LH}} \cdot \frac{P_{GT}(t)}{\eta_{GT}} \tag{6}$$

In the equation, $C_f(t)$ represents the fuel cost at time t; C_{fuel} denotes the cost of fuel, typically priced per unit of energy (e.g., per kilowatt-hour); and V_{LH} refers to the Lower Heating Value of the fuel, indicating the energy released per unit of fuel during complete combustion.

$$C_e(t) = \sum_{k=1}^{n} (C_k \cdot Q_k) \cdot P_{GT}(t) \tag{7}$$

In the equation, $C_e(t)$ represents the pollutant treatment cost at time t; C_k denotes the cost coefficient for treating the k-th type of pollutant; Q_k is the emission amount of the k-th pollutant produced by the micro gas turbine during operation; and n represents the total number of pollutant types.

2.4 Energy Storage Batteries Modeling

Energy storage systems (ESS) play a critical role in microgrids by balancing the disparity between power generation and load demand, optimizing power utilization, and enhancing grid stability and reliability. ESS stores excess electricity and releases it during peak load periods or when renewable energy sources, such as wind or PV systems, have insufficient output. Common types of energy storage batteries include lithium-ion, lead-acid, and sodium-sulfur batteries, among which lithium-ion batteries are widely used in microgrid systems due to their high energy density and long lifespan [37–41].

Energy storage batteries operate by storing electrical energy during the charging process and releasing it back to the grid during discharge. The efficiency of an ESS is closely related to factors such as battery charge/discharge efficiency and lifespan. To effectively manage the charge and discharge processes, a mathematical model is essential for optimizing battery operation strategies [42].

The state of charge (SOC) of a battery represents the ratio of the currently stored energy to the maximum stored energy [43]. The SOC is calculated based on the battery's charge and discharge processes, with its mathematical expression given as follows:

$$SOC(t) = SOC(t-1) + \int_{t-1}^{t} \frac{P_{battery}(t') \cdot \eta_{char} - P_{battery}(t') \cdot \eta_{dischar}}{C_{bat}} dt' \tag{8}$$

In the equation, $SOC(t)$ represents the battery's state of charge at time t, $P_{battery}(t')$ denotes the charging or discharging power during the time interval $[t-1, t]$. η_{char} and $\eta_{dischar}$ are the efficiencies of the charging and discharging processes, reflecting the energy losses in the battery. C_{bat} refers to the total capacity of the battery.

3 Capacity Optimization Strategy

3.1 Objective Function

The planning and design of microgrids need to consider system economics, power supply reliability, and environmental sustainability. This paper aims to minimize the operation and maintenance costs of microgrids, along with environmental and economic costs, by constructing a multi-objective function as

shown in Eq. (9). The objective of the scheduling model is to minimize total costs while maximizing economic and environmental benefits.

$$\min \quad F = \sum_{t=1}^{T} \left(f_{sys} + f_{env} \right) \tag{9}$$

In the equation, f_{sys} represents the operation and maintenance costs of the microgrid system, while f_{env} denotes the environmental and economic costs of the microgrid.

The operational and maintenance costs of the microgrid system

The operational and maintenance costs of the microgrid system consist of three components: the total operational costs of interactions between the microgrid and the main grid C_{GT}, the maintenance costs of energy storage $C_{battery}$, and the total operational costs of micro gas turbines C_{GT}. These components satisfy the following relationship:

$$f_{sys} = \sum_{t=1}^{T} \left(C_{grid}(t) + C_{battery}(t) + C_{GT}(t) \right) \tag{10}$$

(1) Operational and maintenance costs of the power grid system.

The calculation formula is as follows:

$$C_{grid}(t) = p_{buy} \cdot P_{buy}(t) + p_{sell} \cdot P_{sell}(t) \tag{11}$$

where p_{buy} represents the purchase price of electricity, P_{buy} is the purchased power, and their product represents the cost of purchasing electricity from the main grid at time t. Similarly, p_{sell} denotes the selling price of electricity, P_{sell} is the amount of electricity sold to the grid at time t, and their product represents the revenue from selling electricity back to the main grid at time t.

(2) The total operational cost of the micro gas turbine

The calculation formula is as follows:

$$C_{GT}(t) = C_{GTO}(t) + C_{GTM}(t) \tag{12}$$

where $C_{GTO}(t)$ and $C_{GTM}(t)$ represent the operational and maintenance costs and the fuel costs of the micro gas turbine, respectively.

(3) The maintenance cost of energy storage

$$C_{battery}(t) = c_{E,OM} \cdot Q_{E,OM}(t) + c_{P,OM} \cdot W_P(t) + n_{labor} \cdot c_{labor} \tag{13}$$

The calculation formula is as follows:

where $c_{E,OM}$ represents the maintenance cost per unit of energy storage capacity, and $Q_{E,OM}(t)$ is the energy storage capacity (MW·h). Their product represents the capacity maintenance cost. Similarly, $c_{P,OM}$ is the maintenance cost per unit of power capacity, and $W_P(t)$ is the installed power capacity (MW). Their product represents the power capacity maintenance cost. Additionally, n_{labor} is the number of maintenance personnel, and c_{labor} is the annual cost per person, with their product representing the labor operational cost.

(4) Battery degradation cost

In addition to the maintenance costs of the energy storage system, this study further considers battery degradation cost, which reflects the long-term economic impact of battery cycling. The degradation cost is modeled as a function of the cumulative charge and discharge throughput as shown in Eq. (14).

$$C_{\text{deg}} = c_{\text{deg}} \cdot \sum_{t-1}^{T} |P_{ESS,t}| \tag{14}$$

where C_{deg} is the total battery degradation cost ($), c_{deg} is the unit degradation cost ($/kWh), $P_{ESS,t}$ represents the charge or discharge power at time step t, and T denotes the total number of scheduling periods. This degradation model has been widely adopted in recent studies to improve the economic accuracy of long-term energy storage scheduling [44].

The environmental and economic costs of the microgrid system

In microgrid optimization problems, environmental protection costs $C_{env}(t)$ and carbon taxes $C_{tax}(t)$ are two critical cost components, typically used to assess the environmental impact of power system operations. These components satisfy the following relationship:

$$f_{env} = C_{env}(t) + C_{tax}(t) \tag{15}$$

(1) Environmental Protection Costs

Environmental protection costs primarily include the external costs caused by pollutant emissions and energy production methods, such as the combustion of fossil fuels. These costs are typically quantified by the amount of carbon emissions and the corresponding unit cost, such as the environmental cost of carbon emissions. The formula for calculating environmental protection costs can be expressed as:

$$C_{env} = \sum_{t=1}^{T} (\alpha \cdot P_{CO2}(t) + \beta \cdot P_{SO2}(t)) \tag{16}$$

where $P_{CO2}(t)$ represents the carbon dioxide emissions, primarily resulting from the combustion process of gas turbines; $P_{SO2}(t)$ denotes the sulfur oxide emissions from gas turbines; α and β are the environmental cost coefficients corresponding to these pollutants.

(2) Carbon Tax

The carbon tax is a fee imposed by the government on carbon emissions, designed to incentivize the reduction of greenhouse gas emissions through economic measures. The carbon tax is typically calculated based on the amount of carbon dioxide emissions. The formula for calculating the carbon tax can be expressed as:

$$C_{tax} = \tau \cdot \sum_{t=1}^{T} P_{CO2}(t) \tag{17}$$

where C_{tax} represents the carbon tax, τ is the carbon tax rate, and $P_{CO2}(t)$ is the carbon dioxide emissions (in tons) at time t.

Thus, the environmental and economic costs can be expressed as Eq. (18).

$$f_{env} = \sum_{t=1}^{T} (\alpha \cdot P_{CO2}(t) + \beta \cdot P_{SO2}(t)) + \tau \cdot \sum_{t=1}^{T} P_{CO2}(t) \tag{18}$$

3.2 Operational Constraints

(1) Power Balance Constraint

In the microgrid system, the generated power and load demand must remain balanced:

$$P_{wind}(t) + P_{pv}(t) + P_{GT}(t) + P_{battery}(t) + P_{grid} = P_{load}(t) \tag{19}$$

(2) Micro Gas Turbine Output Constraint

The output of the micro gas turbine must remain within its allowable range:

$$\begin{cases} P_{GT}^{\min} \le P_{GT}(t) \le P_{GT}^{\max} \\ |P_{GT}(t) - P_{GT}(t-1)| \le r_{GT} \end{cases} \tag{20}$$

where $P_{GT}^{\min}$ and $P_{GT}^{\min}$ are the minimum and maximum output limits of the micro gas turbine, respectively, and r_{GT} represents the ramp rate limit of the micro gas turbine.

(3) Energy Storage System Constraints

The charging and discharging power, as well as the state of the energy storage system, must satisfy the following conditions:

$$\begin{cases} P_{battery}^{\min} \le P_{battery}(t) \le P_{battery}^{\max} \\ SOC_{\min} \le SOC(t) \le SOC_{\max} \\ \left|P_{battery}(t) - P_{battery}(t-1)\right| \le r_{battery} \end{cases} \tag{21}$$

where $P_{battery}^{\min}$ and $P_{battery}^{\min}$ are the lower and upper limits of the energy storage system's output power, with positive values indicating charging power (input) and negative values indicating discharging power (output). Similarly, $SOC_{\max}$ and $SOC_{\min}$ represent the lower and upper limits of the energy storage capacity. Additionally, $r_{battery}$ represents the ramp rate limit of the micro gas turbine.

(4) Main Grid Power Exchange Constraint

The power exchange with the main grid must remain within its allowable range:

$$P_{grid}^{\min} \le P_{grid}(t) \le P_{grid}^{\max} \tag{22}$$

where $P_{grid}^{\min}$ and P_{grid}^{max} represent the minimum and maximum power exchange with the main grid, respectively.

The optimization strategy for the microgrid, as depicted in Fig. 2, encompasses a comprehensive set of equations and constraints that facilitate the achievement of the objective function outlined in the model.

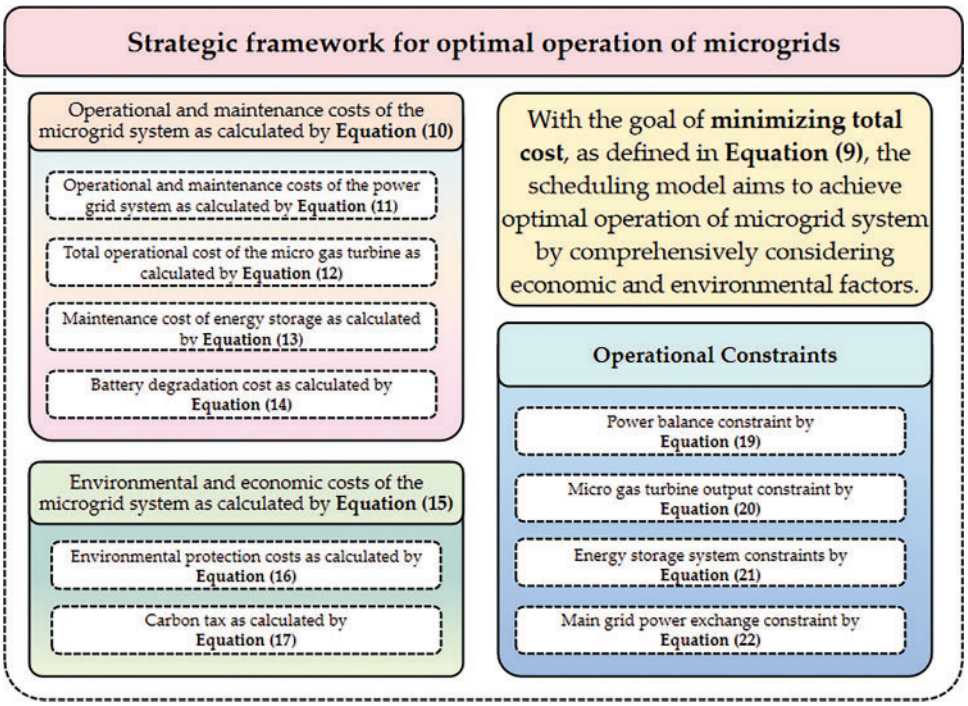

Figure 2: Strategic framework for optimal operation of microgrids

4 Microgrid Optimization Operation Based on DE-HHO

In this section, we have provided a detailed description of the microgrid optimal operation mechanism based on the DE-HHO hybrid algorithm. By integrating the global search capability of DE and the local exploitation capability of HHO, the hybrid algorithm leverages the strengths of both to address complex issues in microgrid optimal scheduling. The DE algorithm generates a diverse population through its mutation and crossover strategies, rapidly covering the solution space to identify potential optimal solutions. In contrast, the HHO algorithm employs its Lévy flight mechanism and dynamic hunting strategies to conduct refined searches in the regions of potential optimal solutions. This combination of mechanisms enables the hybrid algorithm to effectively balance global search and local search capabilities, thereby significantly enhancing optimization performance.

In Section 4.1, we elaborated on the principles of the HHO algorithm, including its characteristics and strategies in the global exploration, transition, and local exploitation phases. In Section 4.2, we analyzed the mutation, crossover, and selection strategies of the DE algorithm, as well as its advantages in the optimization process. In Section 4.3, we described in detail the collaborative mechanism of the DE-HHO hybrid algorithm, including how DE and HHO complement each other in the global exploration and local exploitation phases, and how this collaboration improves the adaptability and robustness of the algorithm.

4.1 Principle of Harris Hawks optimization

With the growing complexity of microgrid systems, traditional optimization algorithms increasingly struggle with multi-objective and multi-constraint optimization problems, exposing limitations such as susceptibility to local optima, insufficient global search capabilities, and low computational efficiency. In response, the HHO algorithm has emerged as a promising intelligent optimization method. Its unique

mechanisms and high efficiency have attracted significant attention, leading to successful applications in microgrid optimization.

Inspired by the cooperative hunting behavior and sudden attack strategies of Harris hawks, HHO combines strong global search abilities with effective local exploitation [45]. The algorithm divides its optimization process into three phases: global exploration, transition from exploration to exploitation, and local exploitation. During global exploration, it simulates random search behaviors to thoroughly explore the solution space and locate potential optima. In the transition phase, the algorithm mimics pursuit behaviors, narrowing the search area and moving closer to optimal solutions. Finally, during local exploitation, it emulates the sudden attack strategy of Harris hawks to refine the solution and achieve high-precision optimization.

Throughout the process, the positions of the Harris hawks represent candidate solutions, while the best solution at each iteration is treated as the prey [46–48]. This innovative structure allows HHO to effectively balance exploration and exploitation, making it a powerful tool for addressing the complexities of microgrid optimization.

Global Exploration Phase

Harris hawks population is randomly distributed across the solution space, performing global searches for the prey (i.e., the optimal solution) using two strategies:

Strategy 1: When the probability $\varphi < 0.5$, each hawk updates its position based on the positions of other members and the prey.

Strategy 2: When the probability $\varphi \geq 0.5$, Harris hawks randomly perch at a location within the population's range.

The position update formulas are as follows:

$$X(t+1) = \begin{cases} \left(X_{prey}(t) - X_m(t)\right) - rand_1 \times \left(lb + rand_2\left(ub - lb\right)\right) & \varphi < 0.5 \\ X_{rand}(t) - rand_3 \times \left|X_{rand}(t) - 2 \cdot rand_4 \cdot X(t+1)\right| & \varphi \geq 0.5 \end{cases} \tag{23}$$

where X_{prey} represents the position of the prey (current optimal solution), X_m is the average position of the current Harris hawks population, ub and lb denote the upper and lower bounds of the search space, and $rand_i$ is a random number in the interval $[0, 1]$.

Transition from Global Exploration to Local Exploitation

The HHO algorithm divides the hunting process of Harris hawks into exploration and exploitation phases based on their predatory habits. As the prey attempts to escape, its energy gradually depletes. The algorithm dynamically selects either exploration or exploitation behavior depending on the prey's escape energy. The prey's escape energy is defined by Eq. (24).

$$E = 2 \cdot E_{initial} \times \left(1 - \frac{t}{T}\right) \tag{24}$$

where $E_{initial}$ represents the prey's initial escape energy, with a value range of $[0, 1]$; t is the current iteration number; and T is the maximum number of iterations. When $|E| \geq 1$, the algorithm enters the exploration phase, while $|E| < 1$ indicates a transition to the exploitation phase.

Local Exploitation Phase

Harris hawks hunt by besieging the prey and launching sudden attacks. However, the prey may escape during the siege, requiring Harris hawks to dynamically adjust their hunting strategies based on the prey's

behavior. To simulate this process, the HHO algorithm incorporates four strategies: soft besiege, hard besiege, soft besiege with progressive rapid dives, and hard besiege with progressive rapid dives.

The selection of these strategies depends on the prey's escape energy $|E|$ and the escape probability r, where r is a random number in the range $(0,1)$, indicating the probability of the prey escaping successfully. If $r < 0.5$, it indicates that the prey has an opportunity to escape; otherwise, the prey is unlikely to escape. Based on $|E|$ and r, the HHO algorithm dynamically adjusts the hunting behavior using the following four strategies:

1. Soft besiege: Strategy when $0.5 \le |E| < 1$ and $r \ge 0.5$

When the prey still has escape ability, Harris hawks adopt a soft besiege strategy to gradually deplete the prey's energy while waiting for the optimal moment to attack. The position update formula is given by:

$$\begin{cases} X(t+1) = \Delta X(t) - E \times \left| J \cdot X_{prey}(t) - X(t) \right| \\ \Delta X(t) = X_{prey}(t) - X(t) \end{cases} \tag{25}$$

where $\Delta X(t)$ represents the difference between the prey's position and the current hawk's position. The introduction of J simulates the random jump intensity of the prey during its escape process. The value of J changes randomly in each iteration to mimic the prey's movement characteristics and is generated as a random number $U(0,2)$ following a uniform distribution.

2. Hard besiege: Strategy when $|E| < 0.5$ and $r \ge 0.5$

When the prey is unable to escape, Harris hawks launch a hard besiege attack to swiftly capture the prey. The position update formula is given by:

$$X(t+1) = X_{prey}(t) - E \times |\Delta X(t)| \tag{26}$$

3. Progressive rapid dive with soft besiege: Strategy when $0.5 \le |E| < 1$ and $r < 0.5$

When the prey has an opportunity to escape but is under gradual pressure, Harris hawks adopt a progressive rapid dive strategy. This involves progressively adjusting their positions and optimizing the attack trajectory. The strategy is implemented using two approaches:

$$Y = X_{prey}(t) - E \times \left| J \cdot \left(X_{prey}(t) - X(t) \right) \right| \tag{27}$$

Harris hawks assess the potential outcome of this movement compared to the previous dive result to determine whether it is an effective dive strategy. If the result is suboptimal (e.g., the prey exhibits more deceptive movements), they switch to the second strategy.

When Harris hawks encounter deceptive behavior from the prey, they employ irregular, sudden, and rapid dive behavior based on the Lévy flight pattern. The mathematical expression for this strategy is as follows:

$$Z = Y + S \times LF(D) \tag{28}$$

where Y is the position calculated based on Strategy 1, S is a random vector of the same dimension as the problem space D, and $LF(D)$ is the Lévy flight function, used to simulate the irregular and rapid diving behavior of Harris hawks. The calculation formula for the Lévy flight function is as follows:

$$LF = 0.01 \times \frac{u \times \sigma}{|v|^{\frac{1}{\beta}}}, \sigma = \left(\frac{\Gamma(1+\beta) \times \sin\left(\frac{\pi\beta}{2}\right)}{\Gamma\left(\frac{1+\beta}{2}\right) \times \beta \times 2^{\beta-1/2}} \right)^{\frac{1}{\beta}} \tag{29}$$

where u and v are random values uniformly distributed in the interval $(0,1)$; β is a default constant, typically set to 1.5; and σ is a constant related to β.

Thus, the final strategy for progressive rapid dive with soft besiege can be expressed by Eq. (30):

$$X(t+1) = \begin{cases} Y & if \quad F(Y) < F(X(t)) \\ Z & if \quad F(Z) < F(X(t)) \end{cases} \tag{30}$$

Through these two strategies, the HHO algorithm can flexibly adjust its hunting approach in response to different behaviors exhibited by the prey. This adaptability enhances the algorithm's global search capability and local exploitation efficiency, leading to improved optimization performance.

4. Progressive rapid dive with hard besiege: Strategy when $|E| < 0.5$ and $\varphi < 0.5$

Although the prey is exhausted, Harris hawks continue to employ the progressive rapid dive strategy to further reduce the distance to the prey, ensuring a successful hunt.

The position update formula for this strategy is similar to that of the progressive rapid dive with soft besiege, and is consistent with Eq. (30) in form. When $F(Z) < F(X(t))$, the update formula for Z is consistent with Eqs. (28) and (29); whereas when $F(Y) < F(X(t))$, the update formula for Y differs from the definition of "progressive rapid dive with soft besiege," and this formula is derived from Eq. (31).

$$X(t+1) = Y = X_{prey}(t) - E \times \left| J \cdot X_{prey}(t) - \frac{1}{N}\sum_{i=1}^{N} X_i(t) \right| \tag{31}$$

The following Fig. 3 illustrates the various strategies employed by the HHO algorithm across different phases.

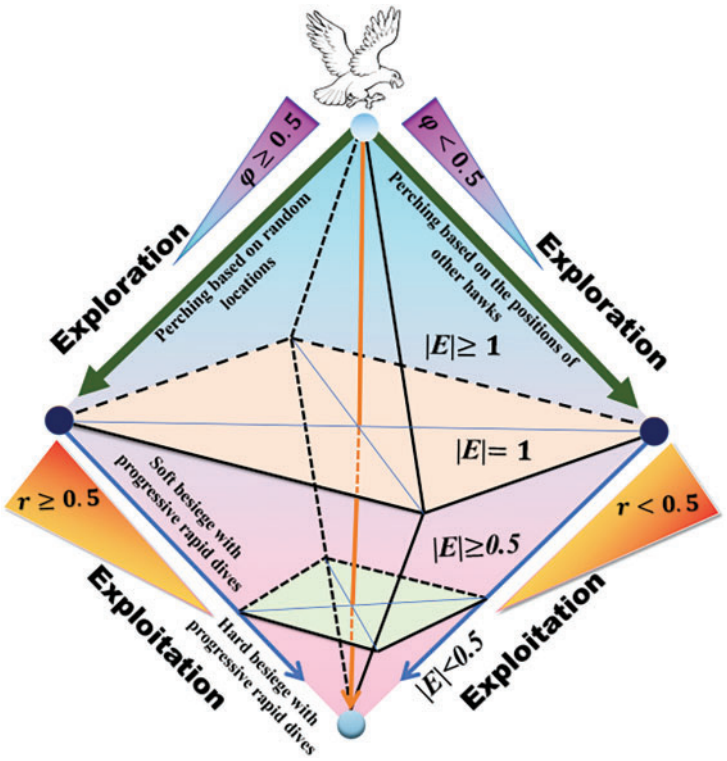

Figure 3: Different phases of HHO

4.2 Principle of Differential Evolution Algorithm

The HHO algorithm is renowned for its unique Lévy flight mechanism and exceptional global search capability, while the DE algorithm holds a prominent position in the optimization domain due to its effective mutation strategies and population diversity maintenance mechanism. Combining the strengths of these two algorithms can result in a novel hybrid optimization strategy aimed at achieving superior optimization performance.

First, integrating DE's mutation strategy enhances population diversity, helping to prevent the algorithm from getting trapped in local optima and thereby improving HHO's global exploration capability. Second, leveraging HHO's Lévy flight mechanism significantly boosts the algorithm's jumping ability, enabling it to escape local optima swiftly. When combined with the DE framework, this further enhances the hybrid algorithm's global optimization performance. Additionally, to better balance the exploration and exploitation capabilities of the algorithm, some studies have introduced multi-strategy approaches (e.g., chaotic strategies, multi-population strategies) in conjunction with DE and HHO to achieve collaborative multi-strategy optimization [49,50]. This hybrid strategy not only retains the advantages of both algorithms but also leverages the complementarity between strategies to improve the algorithm's performance and adaptability in solving complex optimization problems. In the following section, we delve deeper into the working principles of the differential evolution algorithm.

1. Mutation Strategy

In the mutation step, three distinct individuals X_{r1}, X_{r2}, X_{r3} are randomly selected from the population to generate a new solution V_i. Starting from the current solution space, the new solution is calculated using the following expression:

$$V_i = X_{best} + f\left(X_{r1} - X_{r2}\right) \tag{32}$$

$$V_i = X_{it} + V\left(X_{best} - X_{r1}\right) + V\left(X_{r2} - X_{r3}\right) \tag{33}$$

where X_{best} represents the best solution in the current population, and V is the mutation factor that controls the mutation step size.

2. Crossover Strategy

The crossover strategy combines the corresponding mutant vector V_{ij} and target vector X_{ij} to generate a trial vector U_{ij}. The process is governed by the following expression:

$$U_{ij} = \begin{cases} V_{ij} & if\ rand\,(0,1) \le r, j = j_{rand} \\ X_{ij} & else \end{cases} \tag{34}$$

where r is the crossover rate, j_{rand} is a random value in the range $[1, D]$, and D represents the dimensionality of the problem.

3. Selection Strategy

The selection strategy chooses between the trial vector X_i and the target vector U_i based on their fitness values. The selection for the next generation is performed according to the following rule:

$$X_i\left(t\right) = \begin{cases} U_i\left(t\right) & if\ f\left(U_i\left(t\right)\right) \le f\left(X_i\left(t\right)\right) \\ X_i\left(t\right) & else \end{cases} \tag{35}$$

The algorithm selects the individuals for the next generation based on their fitness values. If the fitness value of the trial individual is better than that of the original individual, the trial individual is selected; otherwise, the original individual is retained.

By integrating DE with HHO, an effective hybrid optimization strategy is formulated, which offers several advantages over individual algorithms, as detailed in Table 2.

Table 2: Advantages of the proposed algorithm

Enhanced global search capability	Improved convergence speed	Adaptability to complex optimization problems
The combination of DE's mutation strategy and HHO's Lévy flight mechanism noticeably enhances the algorithm's global exploration ability, enabling it to search the solution space more effectively.	By appropriately designing mutation and crossover strategies, the hybrid algorithm can converge to the global optimum more quickly.	The hybrid algorithm performs exceptionally well in various complex optimization problems, particularly in scenarios requiring a balance between exploration and exploitation.

Thus, through these steps, the DE algorithm effectively explores and exploits the search space to identify the optimal solution to the problem. Fig. 4 illustrates the flowchart of our proposed algorithm.

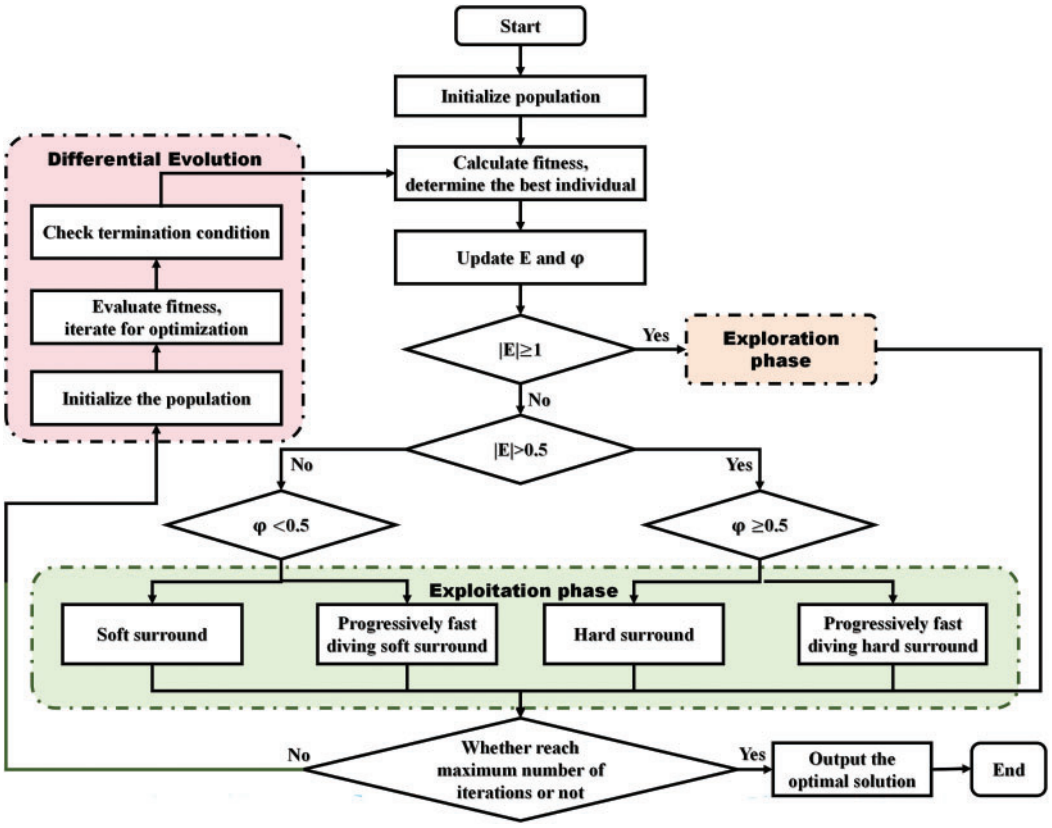

Figure 4: The flowchart of the proposed algorithm

4.3 DE-HHO Collaborative Mechanism

The collaborative optimization mechanism of the DE-HHO hybrid algorithm is reflected in the multi-level complementarity of the algorithm structure. In the initial stage of the algorithm, DE generates diverse candidate solutions through its unique mutation and crossover strategies. By leveraging stochastic search behavior, DE broadly covers the solution space, thereby preventing the algorithm from prematurely converging to local optima. This process provides a rich set of initial solutions for subsequent optimization, thereby enhancing the algorithm's global search capability. Subsequently, the HHO algorithm dynamically adjusts its search strategy based on the prey's escape energy mechanism. It employs Lévy flight and four hunting behaviors to conduct refined searches in the regions of potential optimal solutions. The local exploitation capability of HHO effectively compensates for DE's deficiency in fine-grained search within the solution space, while the population diversity of DE provides better initial solution distributions for HHO. The synergistic effect of these two algorithms significantly improves the convergence speed and optimization accuracy. During the transition from the exploration phase to the exploitation phase, DE's mutation strategy introduces population diversity, effectively preventing premature convergence of the algorithm. The mutation operation of DE involves randomly selecting individuals from the population and introducing new mutation information, thereby maintaining a high level of population diversity throughout the iterative process. This diversity helps the algorithm avoid falling into local optima during the global search phase and provides a broader search space for the local exploitation phase of HHO. By integrating DE's mutation strategy with HHO's dynamic search mechanism, the DE-HHO algorithm can better balance global exploration and local exploitation capabilities, thus demonstrating stronger adaptability and robustness in solving complex optimization problems.

To ensure that the power balance constraint (Eq. (19)) is always satisfied, we have introduced a penalty mechanism to handle constraint violations or infeasible solutions. When a candidate solution generated by the algorithm violates the power balance constraint, we incorporate a penalty term into the objective function to reduce the fitness value of that solution. The magnitude of the penalty term is proportional to the degree of constraint violation, thereby guiding the algorithm to search for feasible solutions that meet the constraint conditions. The calculation formula of the penalty term is shown in Eq. (36).

$$Penalty = \alpha \times \left| \sum P_{gen}(t) - \sum P_{load}(t) \right| \tag{36}$$

where α is the penalty coefficient, which is used to adjust the weight of the penalty term; $P_{gen}(t)$ represents the total power output of all generating units at time t; $P_{load}(t)$ represents the total load demand at time t. Through this approach, the DE-HHO algorithm can effectively avoid generating infeasible solutions and maintain the satisfaction of the power balance constraint throughout the optimization process. This penalty mechanism not only enhances the robustness of the algorithm but also improves the feasibility and reliability of the optimization results.

Moreover, the DE-HHO collaborative mechanism is suitable for addressing model simplification issues in microgrid optimization. In practical applications, due to the complexity of system dynamic characteristics, it is often difficult to construct fully accurate mathematical models. In this study, our model neglects the pitch control dynamics of wind turbines, simplifies the nonlinear characteristics of micro-turbine efficiency variations with load, and assumes a fixed charge-discharge efficiency for energy storage systems, to avoid excessive computational costs that would affect the real-time performance of the optimization algorithm. While these simplifications enhance computational efficiency, they inevitably introduce modeling errors. However, the stochastic nature introduced by the DE-HHO algorithm can effectively cope with the uncertainties arising from such simplifications and provide a certain degree of "compensation." During the global exploration phase, the DE-HHO algorithm employs stochastic search behavior to effectively explore

the solution space and identify potential optimal solutions. This stochasticity can to some extent offset the deficiencies caused by model simplifications, thereby enhancing the adaptability and robustness of the model. Although this approach cannot eliminate the impact of model simplifications, the DE-HHO algorithm can balance global and local search capabilities effectively in the optimization process, thereby mitigating this impact to a certain extent. Experimental results demonstrate that this collaborative mechanism not only improves the robustness of the optimization results but also achieves a good balance between computational efficiency and solution quality.

5 Simulation Results and Analysis

As previously mentioned, this study examines a microgrid system located in an industrial park in the southern region of China, which is composed of wind power generation, photovoltaic (PV) systems, micro gas turbines, and energy storage batteries. The unit parameters of the system are presented in Table 3. Specifically, the maximum power interaction with the main grid, the charge/discharge power of the battery, and the maximum generation power of the gas turbine are all limited to 30 kW. Additionally, negative power values for the battery represent the stored energy in the battery [51]. Furthermore, the power generation of the wind turbine and PV system is influenced by environmental factors and is therefore considered an uncontrollable micro-source, with the rated power reference value used in place of the maximum power. The operating and maintenance (O&M) costs for each distributed generation component are adopted based on empirical values commonly reported in recent literature and industry assessments [52–54].

Table 3: Detailed description of the microgrid system

	WT	PV	MGT	ESS	Load
Minimum power (kW)	0	0	3	−30	50 (off-peak)
Maximum power (kW)	20	40	30	30	90 (on-peak)
Operation and maintenance cost ($/kWh)	0.1195	0.0910	0.3743	0.2114	/

To validate the effectiveness of the proposed DE-HHO in optimizing microgrid tasks, we first constructed models for PSO [51], HHO [29], GWO [55], WOA [56], and the proposed algorithm in the MATLAB R2024a environment. The fitness curves were then compared, as shown in Fig. 5. The y-axis represents the total operational cost of the microgrid system, which is the optimization objective of our study. The parameters for the traditional algorithms are provided in Table 4. Parameter values were determined through grid search and population size and iteration count were kept consistent across all tested algorithms. From Fig. 5, it is evident that DE-HHO converges the fastest, reaching convergence around the 10th generation. In contrast, HHO, PSO, GWO, and WOA tend to get trapped in local optima and take more than 20 iterations to reach their optimal solutions.

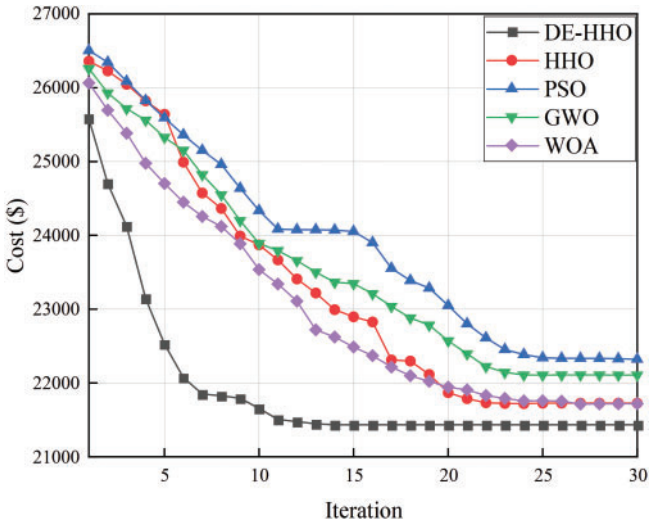

Figure 5: Convergence curves of different algorithms

Table 4: Introduction to parameters of different intelligent optimization algorithms

PSO				
Number of particles (N)	Iteration count	Inertia weight (w)	Self-learning factor (c1)	Social learning factor (c2)
40	30	0.8	2	2
HHO				
Search agent number (N)	Iteration count	The lower limit of the solution space (lb)	The upper limit of the solution space (ub)	
40	30	0	1	
GWO				
Number of wolves (N)	Iteration count	Grid inflation parameter	Leader selection pressure parameter	
40	30	0.1	4	
WOA				
Population size (N)	Iteration count	Probability of encircling mechanism	Spiral factor	
40	30	0.5	1	

Fig. 6 displays the optimal total cost achieved by different optimization algorithms after 30 repetitions of sampling. As shown in Fig. 5, after multiple experiments, the minimum optimal cost reached by DE-HHO is $20,221.37, significantly lower than the $21,184.45 achieved by PSO, $21,372.24 by HHO, $21,291.43 by GWO and $20,687.68 by WOA. Moreover, the maximum optimal cost achieved by DE-HHO is $23,420.55. Despite the existence of extreme values, the distribution of DE-HHO is concentrated around the mean of $21,615.77, which is notably lower than those of the other four optimization algorithms.

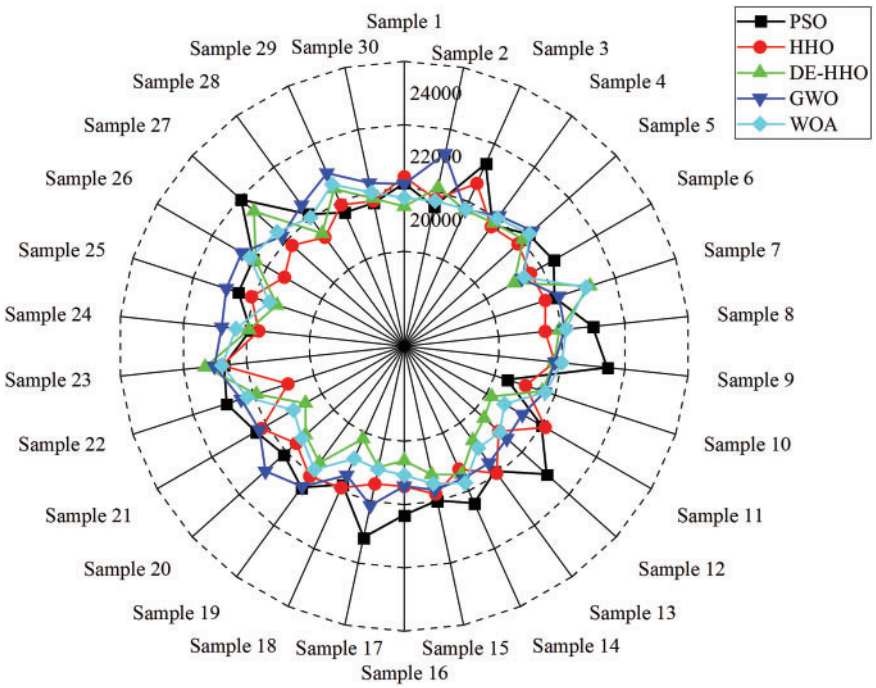

Figure 6: Optimal cost control diagram of different optimization algorithms

Fig. 7 displays the error bars for all compared optimization algorithms. It can be observed that both HHO and DE-HHO exhibit relatively small errors for their optimal values, with little difference between them. However, the average optimal value achieved by DE-HHO is significantly lower than that of HHO. This demonstrates that the DE-HHO algorithm outperforms the others in finding the optimal solution, with the ability to achieve lower cost values, stronger stability, and superior cost control capabilities.

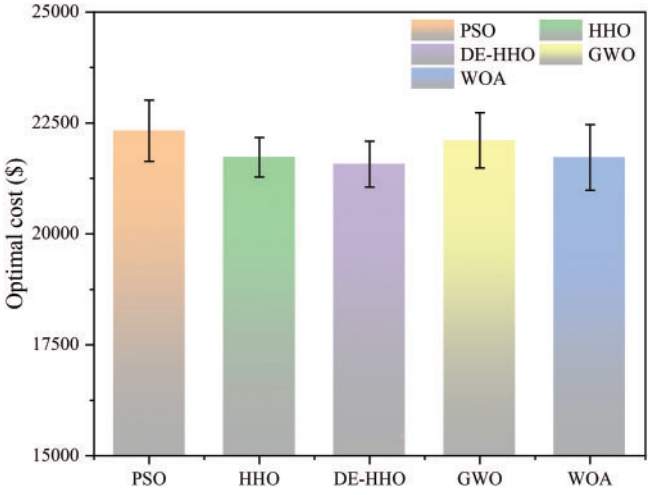

Figure 7: Error bar plot of the optimal solution

In addition to convergence behavior, we also evaluated the computational efficiency of each algorithm. Table 5 presents the average execution time and standard deviation across multiple runs. As shown,

although DE-HHO introduces a hybrid structure, its execution time (90.90 s) remains competitive—only slightly higher than PSO and HHO, and significantly lower than WOA (135.21 s). This demonstrates that DE-HHO achieves a favorable trade-off between optimization performance and computational cost.

Table 5: Execution time of different base algorithms

Algorithm	PSO	HHO	DE-HHO	GWO	WOA
Average execution time (s)	87.83	84.35	90.90	104.47	135.21
Standard deviation	1.28	1.93	1.49	1.57	2.02

To assess the individual roles of DE and HHO in the proposed algorithm, we conducted an ablation study, with results shown in Fig. 8. DE-HHO achieved significantly better best ($20,181.64) and average ($21,573.30) solution values than either DE or HHO alone. Although the worst-case and standard deviation are similar between DE-HHO and HHO, the hybrid approach demonstrates clear optimization advantages. These results highlight a synergistic effect, where the exploration of DE complements the exploitation of HHO. Standalone DE showed the weakest performance.

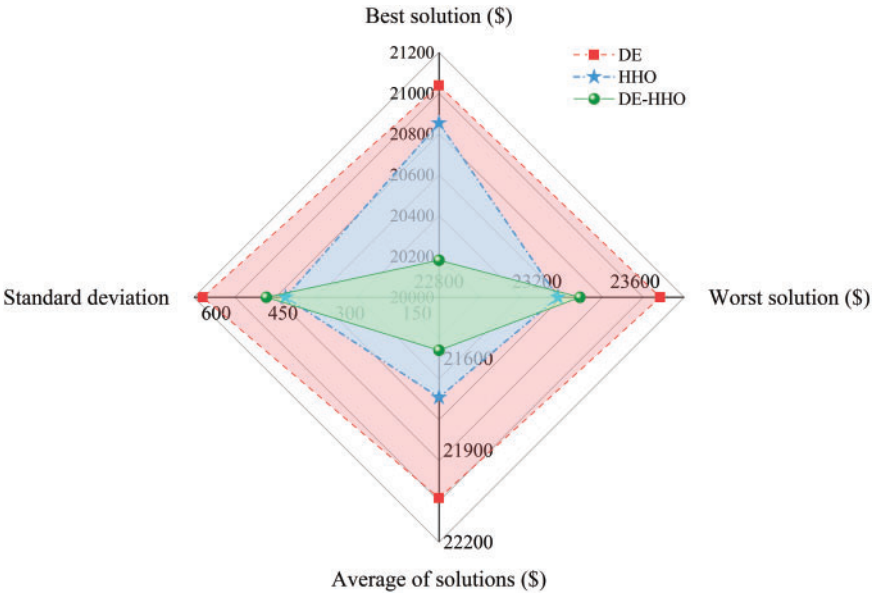

Figure 8: Radar chart of ablation study results

Fig. 9 illustrates the contribution of different DG resources to the microgrid's power supply during each period under the optimized energy management scheme. The load profile of the microgrid is characterized by fluctuating demands throughout the day, with peak loads occurring during the daytime hours (10:00–18:00) and lower demands during the night. Environmental conditions, such as solar irradiance and wind speed, play a crucial role in the generation capabilities of renewable energy sources within the microgrid. The solar irradiance data used in our simulations reflect typical daily patterns, with maximum values occurring around midday (12:00–14:00). Similarly, wind speed profiles show higher values during the early morning and evening hours, which align with common wind patterns in many regions. During periods of high solar irradiance, photovoltaic (PV) systems contribute significantly to the power supply, while wind turbines

provide additional power during the early morning and evening when wind speeds are higher. The micro gas turbines and energy storage systems are utilized to balance the load during peak hours and to ensure a stable power supply when renewable sources are insufficient. Through optimized scheduling, the microgrid can better coordinate the generation and storage strategies of various DG resources to meet electricity demand while minimizing operational costs.

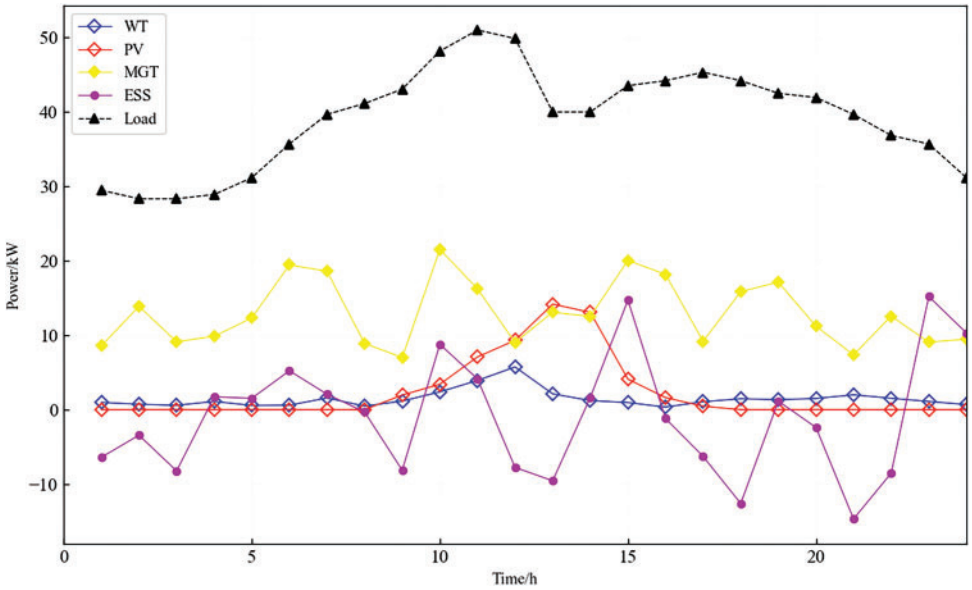

Figure 9: Scheduling results under the DE-HHO strategy

6 Conclusion

This study introduced the DE-HHO optimization strategy for microgrid energy management, which integrates renewable energy sources such as wind, solar, and micro gas turbines, along with energy storage systems. Through comprehensive simulations, the DE-HHO algorithm consistently demonstrated notable performance, outperforming both PSO and HHO in terms of optimal cost efficiency. It achieved the lowest total optimal cost of $20,221.37, significantly reducing operational costs, and exhibited stronger stability and improved cost control compared to the traditional algorithms. The DE-HHO algorithm proved particularly effective in coordinating the operation of distributed generation resources, optimizing both generation and storage strategies to efficiently meet electricity demand.

Despite these promising results, certain limitations warrant attention. The current system modeling simplifies real-world dynamics by omitting factors such as component degradation, ramp rate constraints, start-up/shutdown behaviors, and inverter efficiencies. Incorporating these aspects would enhance the model's realism and applicability. Additionally, the model does not account for uncertainties inherent in renewable energy generation and load demand. Future work should integrate stochastic modeling techniques, such as scenario-based or probabilistic approaches, to better capture these uncertainties by conducting sensitivity and parametric analysis. Moreover, the absence of demand response strategies and dynamic grid interactions limits the model's responsiveness to real-time conditions. Incorporating demand-side management and adaptive control mechanisms could improve system flexibility and resilience. Lastly, the current model lacks dynamic constraints like time-coupling and SOC considerations for energy storage systems. Addressing these factors in future research will contribute to more robust and comprehensive

microgrid optimization frameworks. Furthermore, future studies will aim to validate the proposed method on experimental microgrid platforms to further demonstrate its practical applicability.

Acknowledgement: Not applicable.

Funding Statement: The authors received no specific funding for this study.

Author Contributions: Jingrui Liu: Conceptualization, Software, Data curation, Formal analysis, Project administration, Writing—original draft and Writing—review &editing; Zhiwen Hou: Methodology, Writing—original draft and Writing—review & editing, Formal analysis, Investigation; Boyu Wang: Data curation and Writing—review & editing; Tianxiang Yin: Data curation, Visualization, Supervision. All authors reviewed the results and approved the final version of the manuscript.

Availability of Data and Materials: The data that support the findings of this study are available from the corresponding author upon reasonable request.

Ethics Approval: Not applicable.

Conflicts of Interest: The authors declare no conflicts of interest to report regarding the present study.

References

1. Wang YL, Wang YD, Huang Y, Yu H, Du R, Zhang FL, et al. Optimal scheduling of the regional integrated energy system considering economy and environment. IEEE Trans Sustain Energy. 2019;10(4):1939–49. doi:10.1109/TSTE.2018.2876498.
2. Shaier AA, Elymany MM, Enany MA, Elsonbaty NA. Multi-objective optimization and algorithmic evaluation for EMS in a HRES integrating PV, wind, and backup storage. Sci Rep. 2025;15(1):1147. doi:10.1038/s41598-024-84227-0.
3. Mauludin MS, Khairudin Moh, Asnawi R, Mustafa WA, Toha SF. The advancement of artificial intelligence's application in hybrid solar and wind power plant optimization: a study of the literature. J Adv Res Appl Sci Eng Tech. 2024;50(2):279–93. doi:10.37934/araset.50.2.279293.
4. Ziaee O, Crouchet B, DeBenedicts C. A multi-agent system framework for managing distributed energy resources (DERs). In: Proceedings of the 2025 IEEE Electrical Energy Storage Applications and Technologies Conference (EESAT). IEEE: Charlotte, NC, USA; 2025 Jan 20. p. 1–5.
5. Liu F, Qi S, Wang S, Tian X, Liu L, Zhao X. Robust trading decision-making model for demand-side resource aggregators considering multi-objective cluster aggregation optimization. Energies. 2025;18(2):236. doi:10.3390/en18020236.
6. Opoku K, Dimitrovski A, Ferrari M. Performance evaluation of a novel sequence-based directional detection strategy for protection of active distribution networks. IEEE Access. 2025;13:7094–109. doi:10.1109/ACCESS.2024.3525057.
7. Zeng Y, Hussein ZA, Chyad MH, Farhadi A, Yu J, Rahbarimagham H. Integrating type-2 fuzzy logic controllers with digital twin and neural networks for advanced hydropower system management. Sci Rep. 2025;15(1):5140. doi:10.1038/s41598-025-89866-5.
8. Ahmad Khan A, Faiz Minai A, Godi RK, Shankar Sharma V, Malik H, Afthanorhan A. Optimal sizing, techno-economic feasibility and reliability analysis of hybrid renewable energy system: a systematic review of energy storage systems' integration. IEEE Access. 2025;13(6):59198–226. doi:10.1109/ACCESS.2025.3535520.
9. Saleeb H, El-Rifaie AM, Sayed K, Accouche O, Mohamed SA, Kassem R. Optimal sizing and techno-economic feasibility of hybrid microgrid. Processes. 2025;13(4):1209. doi:10.3390/pr13041209.
10. Thirunavukkarasu GS, Seyedmahmoudian M, Jamei E, Horan B, Mekhilef S, Stojcevski A. Role of optimization techniques in microgrid energy management systems—a review. Energy Strategy Rev. 2022;43(3):100899. doi:10.1016/j.esr.2022.100899.

11. Ahmad Khan A, Naeem M, Iqbal M, Qaisar S, Anpalagan A. A compendium of optimization objectives, constraints, tools and algorithms for energy management in microgrids. Renew Sustain Energ Rev. 2016;58(1):1664–83. doi:10.1016/j.rser.2015.12.259.
12. Zhang T, Hu Z. Optimal scheduling strategy of virtual power plant with power-to-gas in dual energy markets. IEEE Trans Ind Applicat. 2022;58(2):2921–9. doi:10.1109/TIA.2021.3112641.
13. Ren X-Y, Wang Z-H, Li M-C, Li L-L. Optimization and performance analysis of integrated energy systems considering hybrid electro-thermal energy storage. Energy. 2025;314(4):134172. doi:10.1016/j.energy.2024.134172.
14. Nayak CK, Nayak MR, Behera R. Simple moving average based capacity optimization for VRLA battery in PV power smoothing application using MCTLBO. J Energy Storage. 2018;17(1):20–8. doi:10.1016/j.est.2018.02.010.
15. Sultan HM, Mossa MA, Zaki Diab AA, Ouanjli NE. Enhanced techno-economical optimal sizing of a standalone hybrid microgrid power system. In: Mossa MA, Ouanjli NE, Ouaissa M, Dhanaraj RK, editors. Energy conversion systems-based artificial intelligence. Springer Nature Singapore: Singapore; 2025. p. 107–38.
16. Wang Y, Song F, Ma Y, Zhang Y, Yang J, Liu Y, et al. Research on capacity planning and optimization of regional integrated energy system based on hybrid energy storage system. Appl Therm Eng. 2020;180(6390):115834. doi:10.1016/j.applthermaleng.2020.115834.
17. Mehleri ED, Sarimveis H, Markatos NC, Papageorgiou LG. Optimal design and operation of distributed energy systems. In: Computer aided chemical engineering. Vol. 29. The Amsterdam, Netherlands: Elsevier; 2011. p. 1713–7. doi:10.1016/B978-0-444-54298-4.50121-5.
18. Abood S, Ali W, Attia J, Obiomon P, Fayyadh M. Microgrid optimum identification location based on accelerated particle swarm optimization techniques using SCADA system. J Pow Energy Eng. 2021;9(7):10–28. doi:10.4236/jpee.2021.97002.
19. Abualigah L, Sheikhan A, Ikotun M, Zitar A, Alsoud RA, Al-Shourbaji AR, et al. Particle swarm optimization algorithm: review and applications. In: Metaheuristic optimization algorithms. The Amsterdam, Netherlands: Elsevier; 2024. p. 1–14.
20. Zermane AI, Bordjiba T. Optimizing energy management of hybrid battery-supercapacitor energy storage system by using PSO-based fractional order controller for photovoltaic off-grid installation. J Européen Des Syst Autom. 2024;57(2):465–75. doi:10.18280/jesa.570216.
21. Guo S, He Y, Pei H, Wu S. The multi-objective capacity optimization of wind-photovoltaic-thermal energy storage hybrid power system with electric heater. Sol Energy. 2020;195(8):138–49. doi:10.1016/j.solener.2019.11.063.
22. Zhao F, Ji F, Xu T, Zhu N. Jonrinaldi hierarchical parallel search with automatic parameter configuration for particle swarm optimization. Appl Soft Comput. 2024;151(145):111126. doi:10.1016/j.asoc.2023.111126.
23. Jamal S, Pasupuleti J, Ekanayake J. A rule-based energy management system for hybrid renewable energy sources with battery bank optimized by genetic algorithm optimization. Sci Rep. 2024;14(1):4865. doi:10.1038/s41598-024-54333-0.
24. Deng W, Yao R, Zhao H, Yang X, Li G. A novel intelligent diagnosis method using optimal LS-SVM with improved PSO algorithm. Soft Comput. 2019;23(7):2445–62. doi:10.1007/s00500-017-2940-9.
25. Pradhan A, Das A, Bisoy SK. Modified parallel PSO algorithm in cloud computing for performance improvement. Cluster Comput. 2025;28(2):131. doi:10.1007/s10586-024-04722-x.
26. Papadimitrakis M, Giamarelos N, Stogiannos M, Zois EN, Livanos NA-I, Alexandridis A. Metaheuristic search in smart grid: a review with emphasis on planning, scheduling and power flow optimization applications. Renew Sustain Energ Rev. 2021;145:111072. doi:10.1016/j.rser.2021.111072.
27. Deng W, Xu J, Zhao H, Song Y. A novel gate resource allocation method using improved PSO-based QEA. IEEE Trans Intell Transport Syst. 2022;23(3):1737–45. doi:10.1109/TITS.2020.3025796.
28. Marzband M, Yousefnejad E, Sumper A, Domínguez-García JL. Real time experimental implementation of optimum energy management system in standalone Microgrid by using multi-layer ant colony optimization. Int J Elect Pow Ene Syst. 2016;75:265–74. doi:10.1016/j.ijepes.2015.09.010.
29. Heidari AA, Mirjalili S, Faris H, Aljarah I, Mafarja M, Chen H. Harris hawks optimization: algorithm and applications. Future Gener Comput Syst. 2019;97:849–72. doi:10.1016/j.future.2019.02.028.

30. Jiao S, Wang C, Gao R, Li Y, Zhang Q. Harris hawks optimization with multi-strategy search and application. Symmetry. 2021;13(12):2364. doi:10.3390/sym13122364.
31. Liu X, Ma Z, Guo H, Xu Y, Cao Y. Short-term power load forecasting based on DE-IHHO optimized BiLSTM. IEEE Access. 2024;12(17):145341–9. doi:10.1109/ACCESS.2024.3437247.
32. Bilal, Pant M, Zaheer H, Garcia-Hernandez L, Abraham A. Differential evolution: a review of more than two decades of research. Eng Applicatf Artif Intell. 2020;90(1):103479. doi:10.1016/j.engappai.2020.103479.
33. Bade SO, Meenakshisundaram A, Tomomewo OS. Current status, sizing methodologies, optimization techniques, and energy management and control strategies for co-located utility-scale wind–solar-based hybrid power plants: a review. Eng. 2024;5(2):677–719. doi:10.3390/eng5020038.
34. Yu H, Yang X, Chen H, Lou S, Lin Y. Energy storage capacity planning method for improving offshore wind power consumption. Sustainability. 2022;14(21):14589. doi:10.3390/su142114589.
35. Eze VHU, Eze MC, Ugwu SA, Enyi VS, Okafor WO, Ogbonna CC, et al. Development of maximum power point tracking algorithm based on Improved optimized adaptive differential conductance technique for renewable energy generation. Heliyon. 2025;11(1):e41344. doi:10.1016/j.heliyon.2024.e41344.
36. Bendary AF, Ismail MM. Battery charge management for hybrid PV/wind/fuel cell with storage battery. Energy Procedia. 2019;162(4):107–16. doi:10.1016/j.egypro.2019.04.012.
37. Bhuvaneswari S, Mohan A, Sundaram A. Improved BMS: a smart electric vehicle design based on an intelligent battery management system. In: Proceedings of the 2024 International Conference on Inventive Computation Technologies (ICICT). IEEE: Lalitpur, Nepal, 2024 Apr 24. p. 1999–2006.
38. Spitthoff L, Gunnarshaug AF, Bedeaux D, Burheim O, Kjelstrup S. Peltier effects in lithium-ion battery modeling. J Chem Phys. 2021;154(11):114705. doi:10.1063/5.0038168.
39. Rahbarimagham H, Gharehpetian GB. The effect of smart transformers on the optimal management of a microgrid. Elect Pow Syst Res. 2025;238(1):111044. doi:10.1016/j.epsr.2024.111044.
40. Mohapatra S, Sharma S, Sriperumbuduru A, Varanasi SR, Mogurampelly S. Effect of succinonitrile on ion transport in PEO-based lithium-ion battery electrolytes. J Chem Phys. 2022;156(21):214903. doi:10.1063/5.0087824.
41. Monirul IM, Qiu L, Ruby R. Accurate state of charge estimation for UAV-centric lithium-ion batteries using customized unscented kalman filter. J Energy Storage. 2025;107(4):114955. doi:10.1016/j.est.2024.114955.
42. Balasingam B, Ahmed M, Pattipati K. Battery management systems—challenges and some solutions. Energies. 2020;13(11):2825. doi:10.3390/en13112825.
43. Nyamathulla S, Dhanamjayulu C. A review of battery energy storage systems and advanced battery management system for different applications: challenges and recommendations. J Energy Stor. 2024;86(3):111179. doi:10.1016/j.est.2024.111179.
44. Safavi V, Vaniar AM, Bazmohammadi N, Vasquez JC, Keysan O, Guerrero JM. A battery degradation-aware energy management system for agricultural microgrids. J Energy Storage. 2025;108(6):115059. doi:10.1016/j.est.2024.115059.
45. Alabool HM, Alarabiat D, Abualigah L, Heidari AA. Harris hawks optimization: a comprehensive review of recent variants and applications. Neural Comput Appl. 2021;33(15):8939–80. doi:10.1007/s00521-021-05720-5.
46. Shehab M, Mashal I, Momani Z, Shambour MKY, AL-Badareen A, Al-Dabet S, et al. Harris Hawks optimization algorithm: variants and applications. Arch Computat Methods Eng. 2022;29(7):5579–603. doi:10.1007/s11831-022-09780-1.
47. Yang T, Fang J, Jia C, Liu Z, Liu Y. An improved harris hawks optimization algorithm based on chaotic sequence and opposite elite learning mechanism. PLoS One. 2023;18(2):e0281636. doi:10.1371/journal.pone.0281636.
48. Fu L, Zhu H, Zhang C, Ouyang H, Li S. Hybrid harmony search differential evolution algorithm. IEEE Access. 2021;9:21532–55. doi:10.1109/ACCESS.2021.3055530.
49. Zhu L, Ma Y, Bai Y. A self-adaptive multi-population differential evolution algorithm. Nat Comput. 2020;19(1):211–35. doi:10.1007/s11047-019-09757-3.
50. Kamarposhti MA, Shokouhandeh H, Lee Y, Kang S-K, Colak I, Barhoumi EM. Optimizing energy management in microgrids with ant colony optimization: enhancing reliability and cost efficiency for sustainable energy systems. Int J Low Carbon Technol. 2024;19:2848–56. doi:10.1093/ijlct/ctae230.

51. Menzri F, Boutabba T, Benlaloui I, Khamari D. Optimization of Energy management using a particle swarm optimization for hybrid renewable energy sources. In: 2022 2nd International Conference on Advanced Electrical Engineering (ICAEE). Constantine, Algeria: IEEE; 2022. p. 1–5. doi:10.1109/ICAEE53772.2022.9962065.
52. Araoye TO, Ashigwuike EC, Mbunwe MJ, Bakinson OI, Ozue TI. Techno-economic modeling and optimal sizing of autonomous hybrid microgrid renewable energy system for rural electrification sustainability using HOMER and grasshopper optimization algorithm. Renew Energy. 2024;229(3):120712. doi:10.1016/j.renene.2024.120712.
53. Jafari M, Sayyaadi H. Optimal off-grid electricity supply for a residential complex using water-energy-economic-environmental nexus. Energy Convers Manag X. 2025;26(1):100998. doi:10.1016/j.ecmx.2025.100998.
54. He Y, Ge W, Xiao H. Research on optimization of combined heat and power microgrid based on cooperative game. In: Proceedings of the Fifth International Conference on Control, Robotics, and Intelligent Systems (CCRIS 2024). Bellingham, WA, USA: SPIE; 2024 Oct 28. Vol. 13404. doi:10.1117/12.3050474.
55. Mirjalili S, Mirjalili SM, Lewis A. Grey wolf optimizer. Adv Eng Softw. 2014;69:46–61. doi:10.1016/j.advengsoft.2013.12.007.
56. Mirjalili S, Lewis A. The whale optimization algorithm. Adv Eng Softw. 2016;95(12):51–67. doi:10.1016/j.advengsoft.2016.01.008.